Monotonic and cyclic loading of new FRP reinforced concrete cantilever beams

M.Kazem Sharbatdar
Asst. Prof., Dept. of Civil Engineering, Engineering Faculty, Semnan University, Semnan, Iran

Abstract : *FRPs (fiber reinforced polymer) possess many favorable characteristics suitable and applicable for construction industry when compared with steel reinforcement. There are new ideas to use FRPs as longitudinal or transverse reinforcement for new concrete elements particularly for bridge decks or beams. Although high tensile strength of FRP is main characteristic for applications at both areas, its weakness to bending and linear stress-strain behavior with virtually no ductility, makes it vulnerable to probably premature failures under reversal tension-compression loading during earthquake. A pilot research project has been conducted to explore the characteristics of large-scale cantilever concrete beams reinforced with FRP re-bars and grids and were tested under either simulated cyclic loading or monotonically increasing lateral loading. This paper presents the test parameters and results obtained during research. The analytical relationships are compared with those recorded experimentally, and test results showed the diagonal cracks and either rupturing of FRP bars in tension or stability failure in compression bars at long or short shear span beams. The comparison of nominal moment capacities between analytical and experimental values confirms that plane section analysis is applicable to FRP reinforced concrete members.*

Keywords: *Beams, Shear and Flexural Behavior, Monotonic Loading, Fiber reinforced polymers (FRP), Longitudinal re-bars, Transverse Grids, Ductility, Plane Section Analysis*

1. Introduction

The use of fiber reinforced polymer (FRP) reinforcement in new concrete construction is currently being explored as an innovative construction material. The major driving force behind this effort is the superior performance of FRPs in corrosive environments. FRPs possess high strength-to-weight ratio, favorable fatigue strength, and low relaxation characteristics when compared with steel reinforcement, offering economically and structurally sound alternative in most applications. They also have high electro-magnetic transparency. An important feature for structural applications is its high strength, while exhibiting linearly elastic stress-strain characteristics with virtually no ductility. Few pilot projects have been implemented in actual practice involving the use of FRP re-bars and grids in concrete beams, bridge decks and slabs. The behavior of bars in tension-compression reversals, as in the case of reinforcement in earthquake resistant elements, has not yet been explored. Furthermore, the inherent brittleness of FRP reinforcement poses challenges for seismic applications from the point of view of energy dissipation through plastic hinges. The use of FRP transverse reinforcement presents additional challenges, as shear resistance has not been well established.

Nagasaka and Fukuyama (1993) carried out several tests on simply supported beams reinforced with steel longitudinal bars and FRP stirrups, it was conducted that increase in stirrup ratio, rw improved the stiffness reduction by controlling diagonal cracking increased the ultimate shear capacity. The experimental investigation conducted by Grira and Saatcioglu (2000) indicated that FRP grids could be used as column confinement reinforcement for improved seismic performance. Nagasaka et al. (1993) test results showed that the ultimate shear capacity of the beams was determined by tensile breaking of stirrups or crushing of diagonal compression struts and also the shear capacity of the beams depended on the amount and type of FRP used. Zhao and Maruyama (1995) during their research found that the longitudinal reinforcement ratio, rt, did not have a considerable influence on shear capacity and the results were consistent with what might be predicted by current codes. Kawai et al. (1991) and Nakano et al (1993) and

[Downloaded from ijce.iust.ac.ir on 2024-07-23]

Weichen (2001) separately at their research showed that bending characteristics of FRP reinforced concrete beams could be predicted by using the plane-section analysis as conventional method used for steel-reinforced concrete members so long as the yield strength of reinforcement is replaced by a rational value for FRP strength.

2. Research Significant

Very little research has been conducted on the behavior of FRP reinforced concrete beams to lateral load reversals, instead most of researches on applications of FRP re-bars were at beams loaded statically and monotonically. R.Salib et al. (2001) presented a comprehensive analytical model to evaluate the strength of concrete beams reinforced with FRP bars and the corresponding modes of failure, including the pre-mature failure of beam due to dowel failure. Meng et al. (2001) presented a method to determine upper and lower limits of reinforcement ratio for CFRP reinforced concrete beams. The lower limit was based on the assumption of crushing concrete prior to the failure of FRP failure but the upper limit of reinforcement ratio is determined based on the failure occurs in CFRP bars. Previous research indicated that the majority of design code provisions for steel reinforced concrete are also applicable to FRP-reinforced concrete, so long as appropriate allowable stresses are used for tension and compression capacities of FRP reinforcement. Japanese Design Guideline of FRP Reinforced Concrete (1997), Canadian Standards Association S806-02 (2002), recommended strain compatibility analysis for the analysis of FRP-reinforced members in flexure.

Since there was limited experimentally work on the behavior of concrete beams reinforced with FRP bars and evaluate the tensile and compressive strength of these FRP bars as main characteristic for applications of statically and reversal loading cases, a research project including several phases has been conducted to explore the characteristics of large-scale cantilever concrete beams reinforced with FRP re-bars and grids and were tested under either simulated cyclic loading or monotonically increasing lateral loading. And also the analytical works were done to find relationships in order to be comparer with those recorded experimentally.

3. Experimental Research

3.1. Test Specimens and Setup

A total of six full-size cantilever beams, representing a portion of a continuous beam between a fixed end and the point of inflection were designed, built and tested. The beams were tested in the vertical position, either under monotonically increasing lateral loading or simulated seismic loading consisting of deformation reversals. The geometry of beam specimens is illustrated in Figure 1. The specimens had 305 mm wide and 405 mm deep cross-section with totally 10 bar arrangements. A total of 6 - 9.5 mm diameter Pultrall CFRP bars were used as top (negative) beam reinforcement and 4 same size bars were used as bottom (positive) reinforcement. These arrangements were resulted in 0.39% and 0.26% as top and bottom reinforcement ratios, respectively. Two different lengths were used; 1000 mm, and 1900 or 1980 mm, corresponding to shear spans of 870 mm and 1780 or 1870 mm, respectively, measured to the point of application of lateral force. The longer shear span was intended to promote flexural behavior while the shorter span would promote shear failure. Four specimens were tested under reversed cyclic loading and two other companion specimens were tested under monotonic lateral loading. The actual average cylinder strength obtained at the time of testing was 40 MPa. The CFRP transverse reinforcement, grids, was placed either at 180 mm spacing (corresponding to d/2) or 90 mm spacing (corresponding to d/4). Table 1 provides a summary of beam properties and test parameters.

The average tensile strength and modulus of elasticity of CFRP bars were 1450 MPa and 122,000 MPa, respectively. Figure 2 illustrates

[Downloaded from ijce.iust.ac.ir on 2024-07-23]

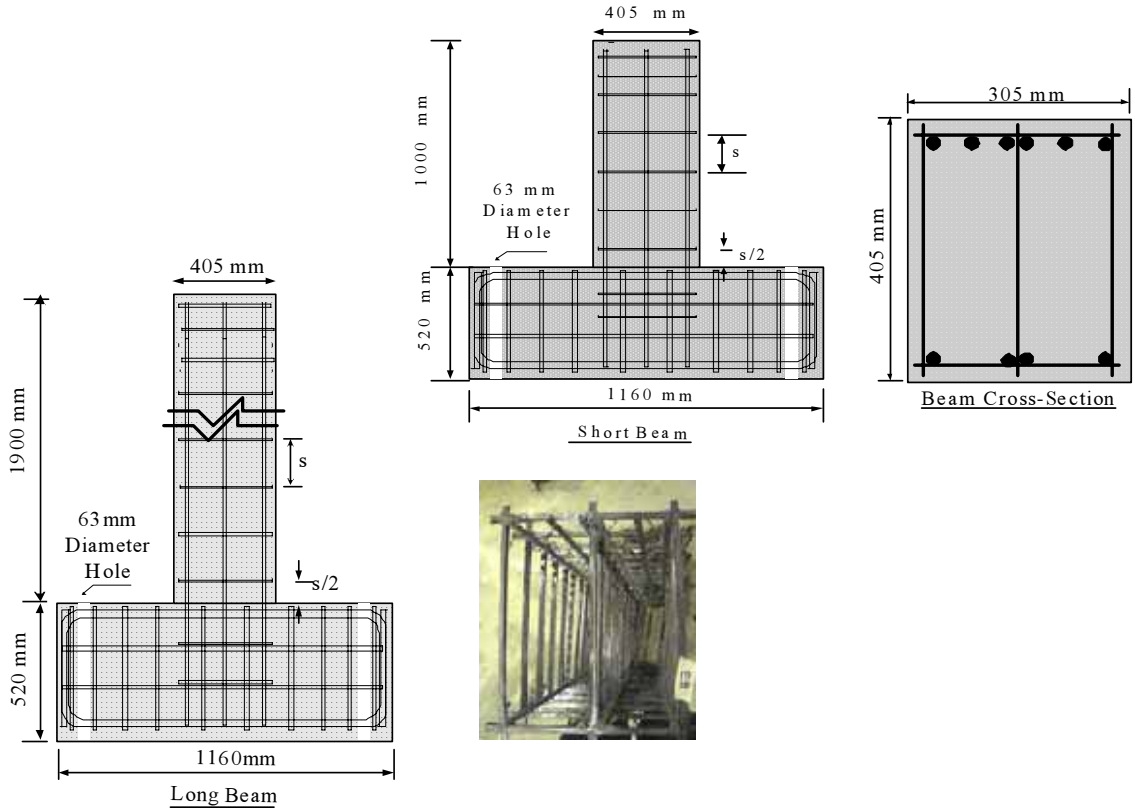

Fig.1 Geometry of Cantilever Beams

Table 1 Properties of Beams under Reversed Cyclic and Monotonic Loading

Specimen Label	f'_c (MPa)	Reinf Arrang.	ρ (%) (strong-side)	ρ (%) (weak-side)	s (mm)	L (mm)
CFB1	35	10-9.5 mm bar	0.39	0.26	175	1000
(A_F=6-9.5 mm at top side & A'_F=4-9.5 mm at bottom side of beam) ($\rho=A_F/bd$, $\rho'=A'_F/bd$)						
CFB2	35	10-9.5 mm bar	0.39	0.26	88	1000
CFB3	35	10-9.5 mm bar	0.39	0.26	88	1000
CFB4	35	10-9.5 mm bar	0.39	0.26	175	1900
CFB5	35	10-9.5 mm bar	0.39	0.26	88	1900
CFB6	35	10-9.5 mm bar	0.39	0.26	88	1900

[Downloaded from ijce.iust.ac.ir on 2024-07-23]

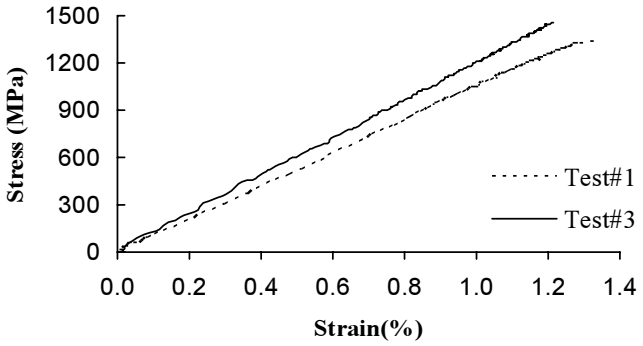

Fig.2 Tensile Stress-Strain Relationship of Pultrall CFRP Bars

the tensile stress-strain relationship of bars tested at the lab; it shows linear behavior up the rupture load. The tensile strength of these was approximately 4 times that of steel bars. The transverse reinforcement used consisted of NEFMAC CFRP grids. The grids had a rectangular configuration with 250 x 350 mm out-to-out dimensions. Two types of grids were employed; i) 6 x 8 mm rectangular cross-section forming two equal-size rectangular openings, and ii) 8 x 10 mm rectangular cross-section forming two equal-size rectangular openings.

The beams were prepared along with attached reinforced concrete elements, representing the framing columns. These elements were used to fix the beams to the laboratory strong floor to provide full fixity. The instrumentation consisted of LVDTs for displacement and rotation measurements, and electric resistant strain gauges for reinforcement strain measurements. The strain gauges were placed on longitudinal and transverse reinforcement. A 1000 kN capacity servo controlled MTS actuator was used to apply the lateral load directly on the beams, no axial load was applied to the beams. A steel box section was attached to a steel plate by means of dwydag pre-stressing bars and used to apply the load. The assembly was first secured near the tip of beams. The detail of test set-up, photographs, and locations of LVDTs are illustrated in Figure 3.

3.2. Observed Behavior and Test Results

Observed behavior of beams such as photographs taken during testing and also test results in terms of hysteretic and monotonic relationships are presented and discussed in this section. The hysteretic behavior is presented both in terms of force-displacement, moment-drift, moment-total rotation relationships. Rotation readings were taken within the potential hinge region. The hinging region was defined as the beam segment between the beam-column (footing) interface and the section 405 mm away from the interface (equal to the longer cross-sectional dimension). The first set of readings gave total rotation of assumed hinging region relative to the column. This set of readings consisted of rotations mostly due to flexure and also due to anchorage slip. The rotations due to the anchorage slip were measured and formed the second set of readings. These readings were taken as the rotation of a beam section near the beam-column interface, relative to the column. Ideally, these readings should have reflected the rotation of the critical beam section at the interface. However, the LVDTs used required some gauge length to be positioned on the beam. Hence, they were mounted on a section approximately 25 mm above the interface. The difference between the total and anchorage slip rotations gave those caused by flexure.

The variations of reinforcement strains in longitudinal and transverse reinforcement are presented in the form of hysteretic force-strain relationships. Each beam had four longitudinal bars instrumented with a total of 6 strain gauges to measure the variation of strain in CFRP bars. All four corner bars were instrumented at the

[Downloaded from ijce.iust.ac.ir on 2024-07-23]

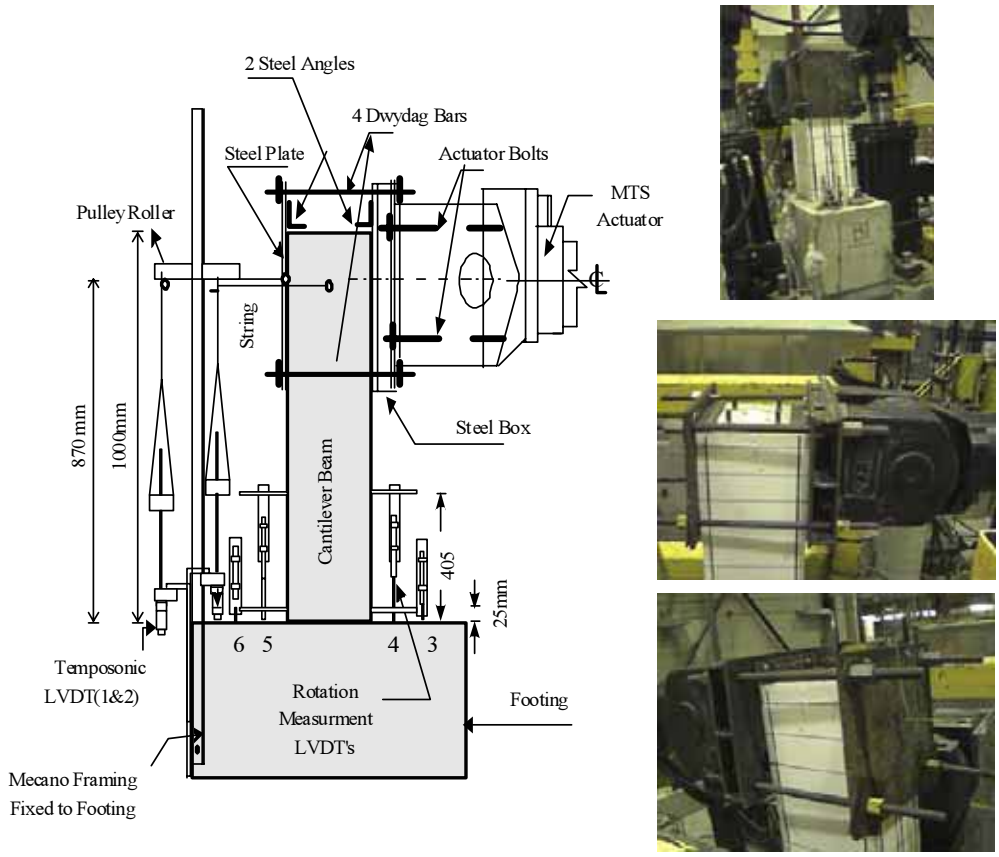

Fig.3 Locations of LVDT's and the Test Setup for Beams

critical beam section, at the interface with the attached (column) element. Two additional strain gauges were placed on one of the negative reinforcement bars in the corner to monitor the variation of strains; one gauge was placed at 175 mm away from the column and the other at 175 mm inside the column. The end grids (closer to the columns) were instrumented with strain gauges, as well. Beams with d/2 grid spacing had the first three grids instrumented, while those with d/4 spacing had the first four instrumented. The amount and spacing of grid reinforcement as an important considered parameter varied in test beams. These test parameters are expressed relative to those required by CSA S806-02. Therefore, a summary of these requirements is presented below. CSA S806-02 shear design requirements are based on 45-degree truss analogy with contributions from concrete and FRP reinforcement. Accordingly, the concrete shear resistance, V_c, without considering reduction factors, is calculated at two different expressions as follows:

$$V_c = \left(\frac{130}{1000 + d}\right) \sqrt{f_c'}\ b_w\ d \le 0.08 \sqrt{f_c'}\ b_w\ d \quad (1)$$

$$0.1\sqrt{f_c'} b_w d \le V_c = 0.035 \left(f_c' \rho_w E_F \frac{V_f}{M_f} d \right)^{1/3} b_w d \le 0.2\sqrt{f_c'} b_w d \quad (2)$$

Equation (1) is for sections with an effective depth greater than 300 mm and with transverse shear reinforcement less than minimum amount of shear reinforcement, b_W and d Equation (2) also is for sections having either at least the minimum amount of transverse reinforcement or an effective depth not exceeding 300 mm. and are effective web width and effective depth of section, respectively. f'_c and E_F are cylinder compressive strength of concrete and modulus of elasticity of FRP bar in tension. Longitudinal reinforcement ratio, ρ_W, is equal to ($\frac{A_{frp}}{b_w \cdot d}$).V_F

[Downloaded from ijce.iust.ac.ir on 2024-07-23]

Fig.4 Observed Damages in Beam CFB1

and M_F are respectively factored shear and moment resistance calculated in accordance with ultimate limit state design. Other parameters are ϕ_F,Capacity reduction factor for FRP reinforcement; A_V, Area of shear reinforcement perpendicular to the axis of member within distance s, and f_{FU}, Ultimate strength of FRP shear reinforcement.

In all the beams tested, applied shear forces, V_r corresponding to flexural capacities were higher than the concrete shear resistance, V_c, therefore, shear reinforcement was required in all beams. The required area of shear reinforcement, A_F, in CSA S806-02 is specified below.

$$V_F = \frac{A_F \phi_F f_{FH} d}{s} \tag{3}$$

Where S and f_{FH} are spacing and maximum tensile strength of FRP transverse reinforcement, respectively. The maximum spacing of transverse shear reinforcement is limited by CSA A23.3-1994 to 0.7d or 600 mm for members subjected to shear stresses of lower than 0.1 $\lambda\varphi_c f'_c$, which is the case for the tested beams. The same spacing limit is specified as 16 times the longitudinal bar diameter, 48 times the minimum cross-sectional dimension of FRP grid, the least dimension of the compression member, or 300 mm for the stability of compression reinforcement. Furthermore, the confinement requirements for seismic design limit the spacing to d/4 or 150 mm, whichever is smaller. The minimum amount of shear reinforcement required is;

$$A_v = \frac{0.3\sqrt{f'_c} b_w s}{f_{FH}} \tag{4}$$

All long and short beams except CFB1 were able to develop their flexural strengths. Beam CFB1 was a short shear dominant beam, reinforced with grids of totally 240 mm^2 cross-section and 180-mm spacing. The spacing was less than the maximum limit of 0.7d = 255 mm for shear, but higher than the maximum limit of d/4 = 90 mm for confinement, though it was closer to the bar stability limit of 16 times the diameter of longitudinal bar, which came out to be 150 mm. The amount of transverse reinforcement was approximately 33% more than that specified by Equation (3) as required reinforcement for shear, but 22% below the minimum amount required by the CSA S806-02, Equation (4). The beam showed nearly elastic behavior up to about 2.2% drift ratio under reversal loading, with some stiffness degradation caused by concrete cracking. However, the beam developed a wide diagonal tension crack between the first and the second grid form the column face, when it was loaded to 2.5% drift level in the strong direction. Widening diagonal crack completely diminished concrete contribution to shear, putting significant shear on the compression bars, forcing them to resist dowel forces, and developed stability failure and broke, as shown in Figure 4. The reversal of the beam had no flexural resistance left in the weak direction since the tension reinforcement had all but failed during the previous loading in the opposite direction. This is

[Downloaded from ijce.iust.ac.ir on 2024-07-23]

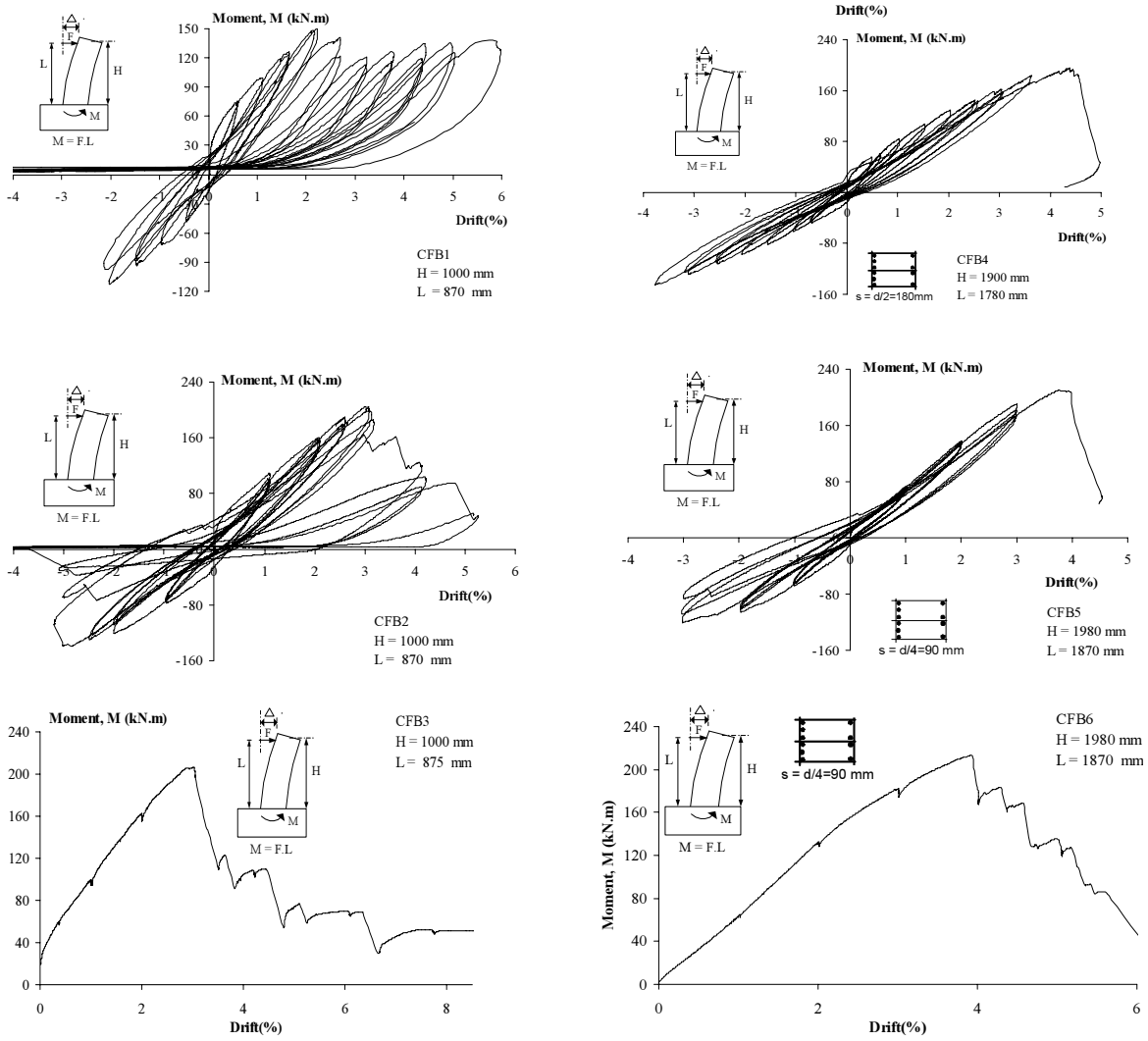

Fig.5 Hysteretic Behavior of Beam

(a) Beam CFB5 (b) Beam CFB6

Fig.6 Observed Damages in Beams CFB5 and CFB6

[Downloaded from ijce.iust.ac.ir on 2024-07-23]

evident in the hysteretic relationship shown in Figure 5. Beam CFB2 was companion to CFB1, except for the grid spacing, which was reduced to 90 mm. This level of spacing is consistent with the spacing requirement for confined concrete, specified in CSA S806 for seismic design. It also meets the maximum spacing requirements for shear and stability of longitudinal compression bars. The reduction in grid spacing increased the effectiveness of shear resistance while enhancing concrete confinement, and developed its flexural strength. The hysteresis loops showed near elastic behavior with some stiffness degradation due to concrete cracking up to 3% drift ratios. Degradation of strength began at the first cycle of 3% drift, and continued till 4% drift ratio. At this level of deformation, all the 4 positive bars ruptured in tension causing the beam to loose its flexural resistance in the weak direction. The beam was able to resist severely reduced loading in the strong direction when pushed to 5% drift before the rupturing all negative bars and then ending test. Beam CFB3 was identical to beam CFB2, except it was tested under monotonically increasing lateral loading. The results showed that both Beams CFB2 and CFB3 had approximately the same primary (envelope) force-deformation relationship. The beam showed increasing load resistance up to 3% drift, followed by subsequent strength decay beyond this deformation level due to the failure of FRP bars in tension. The strength decay continued gradually up to 6% drift ratio with a clear reduction in load resistance every time there was bar rupture in tension.

Beam CFB4 was companion to CFB1, except for its longer length of 1900 mm with promoting the flexural behavior. The hysteretic relationship indicates that the beam showed stable hysteresis loops up to 3.5% drift ratio, but developed significant strength decay after the first cycle of 4 % drift ratio. The beam failed during the first cycle at 4.5 % drift ratio due to the failure of FRP bars in tension. Beam CFB5 was identical to CFB4, except for the spacing of grids, which was reduced to 90 mm. Hysteresis loops indicate stable behavior up to 2% drift ratio, for loading in both directions. Figure 6 shows the beams CFB5 and CFB6 at the end of test, Beam CFB6 was identical to beam CFB5, except it was tested under monotonically increasing lateral loading in the strong direction. The results showed that both Beams CFB5 and CFB6 had approximately the same primary (envelope) force-deformation relationship. The beams showed increasing load resistance up to 4% drift, followed by subsequent strength decay beyond this deformation level due to the failure of FRP bars in tension. The strength decay continued gradually up to 6% drift ratio with a clear reduction in load resistance every time there was bar rupture in tension.

Strain gauge readings of beams indicated that all negative FRP bars ruptured in tension at strains 1.15% to 1.4%, but compressive bars experienced 0.15% to 0.3% strain. FRP grids experienced a tensile strain of 0.3% to 0.5%. Figures 7 and 8 show the hysteretic behaviors of strains in bars and grids, respectively.

3.3. Effects of Test Parameters

Parameters affecting shear and also effect of cyclic loading were as main test parameters. The specimens were designed with two shear spans and two spacing of transverse shear reinforcement to investigate the shear behavior of FRP reinforced beams. While beams with short shear span would be subjected to higher shear stresses, those with closely spaced transverse grids would have higher shear capacity. Beams CFB1 and CFB2 had short shear spans with two difference spacing of grid reinforcement. Beam CFB1 developed a wide diagonal tension crack due to shear. The spacing of grid reinforcement had been reduced by 50% in CFB2, resulted in the doubling of the amount of shear reinforcement. The beam did not suffer from shear failure, and behaved in the flexure mode despite its short shear span, developing 37% higher shear resistance. This is evident in Figure 9 where the envelopes of hysteretic force-deformation relationships are compared.

The comparison of long beams CFB4 and CFB5 with different grid spacing does not show any significant difference in behavior. This is expected since these beams behaved

[Downloaded from ijce.iust.ac.ir on 2024-07-23]

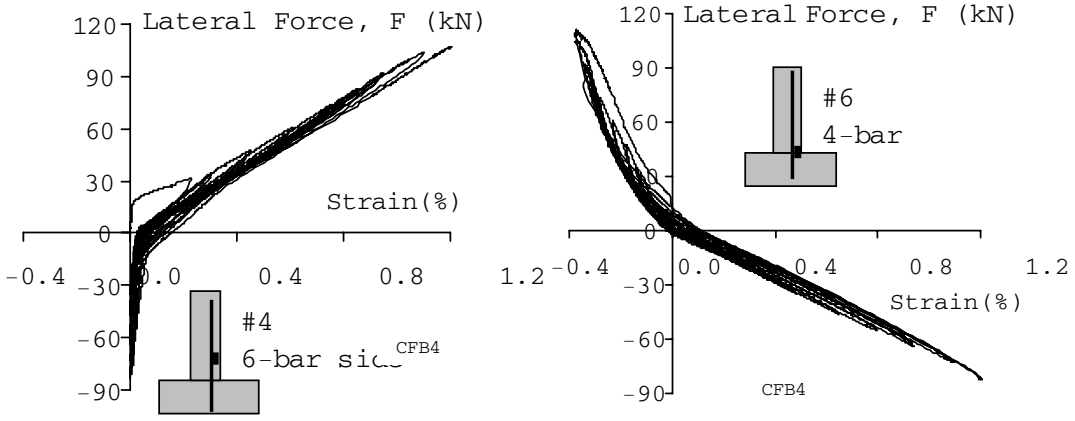

Fig.7 Bar Strain Readings in Beams

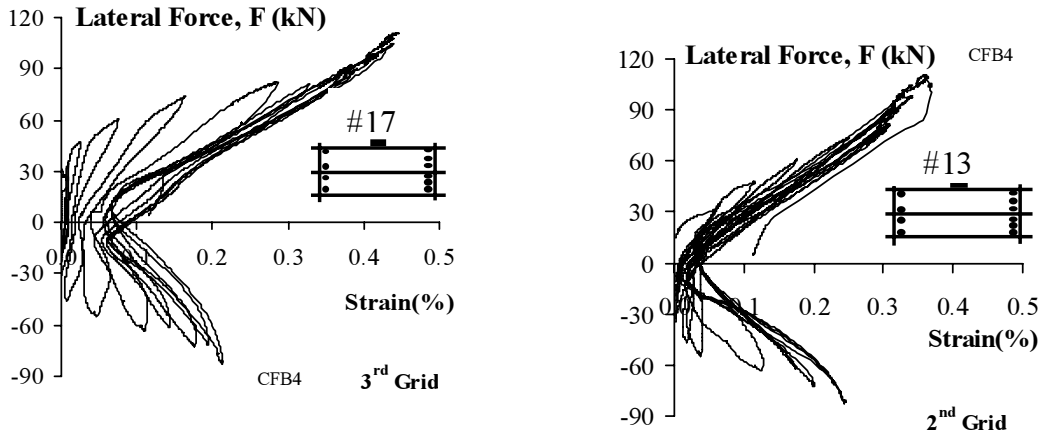

Fig.8 Grid Strain Readings in Beams

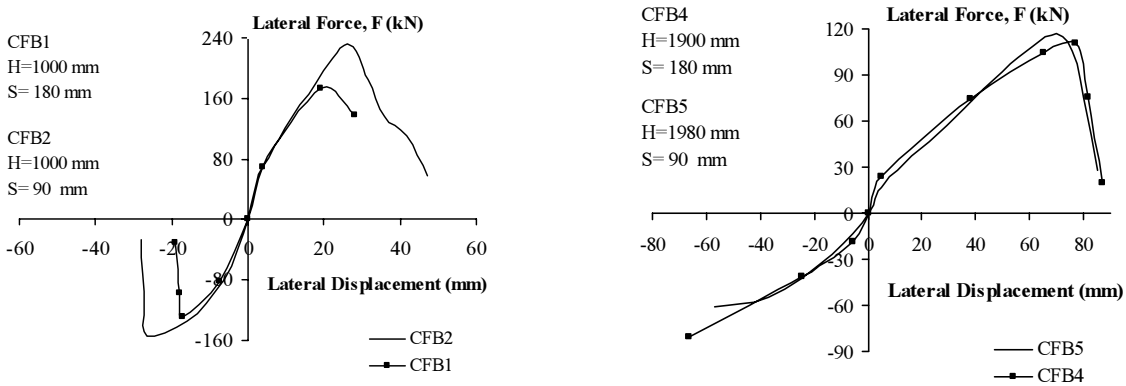

Fig.9 Comparison of the Beams for effect of Spacing of Grids

[Downloaded from ijce.iust.ac.ir on 2024-07-23]

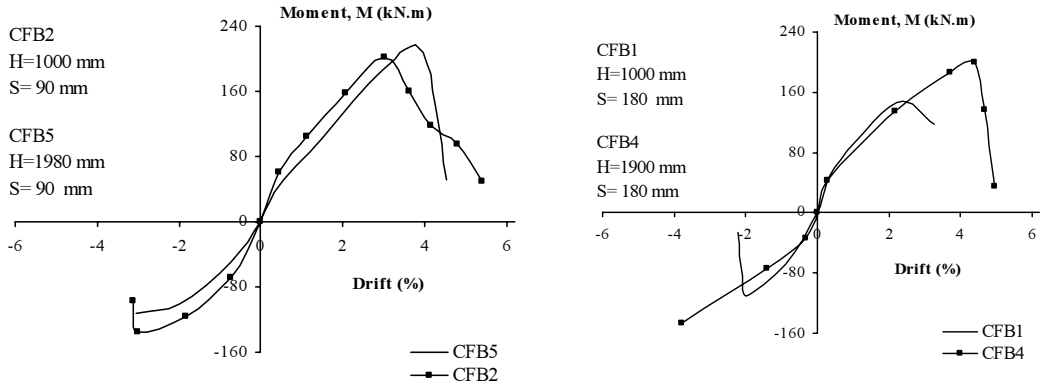

Fig.10 Comparison of the Beams for effect of Shear Spans

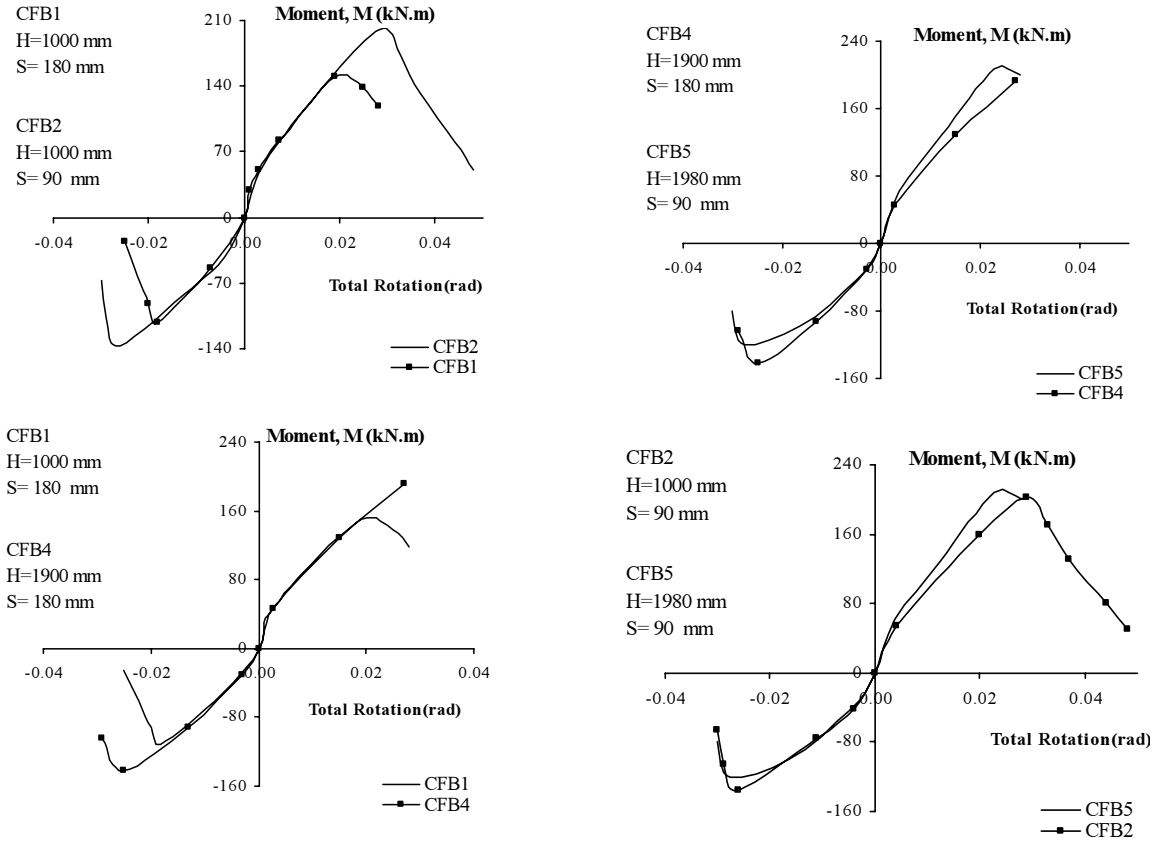

Fig.11 Moment-Total Rotation Relationships of Beams

predominantly in the flexure more because of their longer shear spans. Figure 10 shows envelope curves of moment-drift relationships for beams with different shear spans. Of significance is the comparison of CFB1 and CFB4, both with wide grid spacing. The figure indicates that CFB1, with a short shear span was subjected to higher shear stresses and suffered premature shear failure, whereas CFB4, with the same grid spacing was able to develop its flexural strength without shear failure. Figure 11 also indicates that flexural rotations measured in CFB2 were 70% and 36% higher than those of CFB1 in the strong and weak directions, respectively. Two of the beams, CFB3 and CFB6 were tested under monotonically increasing

[Downloaded from ijce.iust.ac.ir on 2024-07-23]

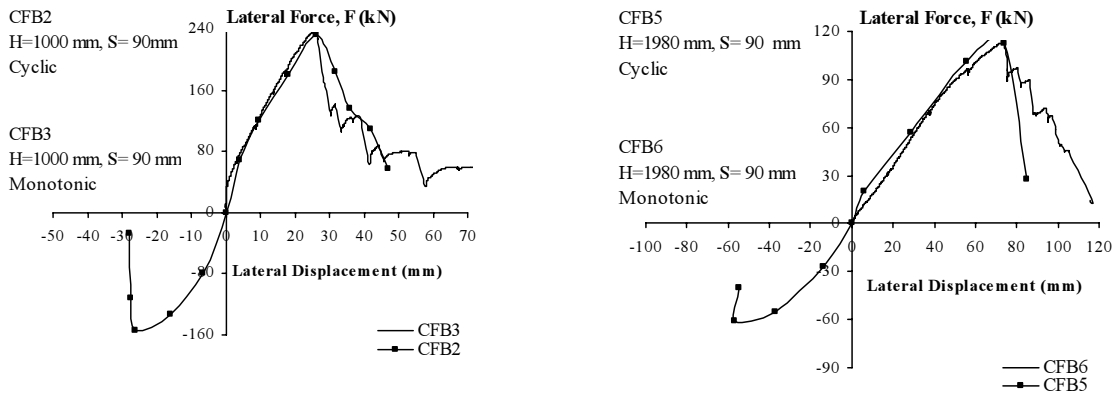

Fig.12 Comparison of the Beams for Effect of Cyclic Loading

lateral loading, while all others were tested under reversed cyclic loading. Each of these two beams had a different shear span, but the same reinforcement, including the same spacing of transverse grids. Comparing CFB2 could see the effect of cyclic loading and CFB3 with short shear spans and CFB5 and CFB6 with long shear spans. The envelope curves for these four beams are presented in Figures 12. The results indicate that the monotonic force-deformation relationships are similar to the envelopes of hysteretic relationships obtained under cyclic loading, suggesting very little or no effect of cyclic loading on beams.

4. Analytical Predictions

Analytical work has also been limited due to lack of data and proper understanding of FRP reinforced concrete behavior. Therefore, analytical research was done in this research based on the experimental data in order to examine and re-assess of applicability of current analytical techniques intended for steel reinforced concrete structures to FRP reinforced concrete structures. Flexural behavior of a concrete beam reinforced with steel reinforcement can be established by plane section analysis based on some assumptions. The plane section analysis provides moment resistance of a section for a given strain profile. Different strain profiles may be considered under increasing flexural stress conditions and the variation of sectional moment resistance can be plotted against sectional curvatures. The resulting diagram provides a moment-curvature relationship, which exhibits all the relevant characteristics of a section in terms of strength, stiffness and deformability. A computer program was used to generate analytical moment-curvature and compared with experimental results. An important step in conducting the analyses was the consideration of realistic material models for constituent materials. The stress-strain relationships for unconfined and confined concrete were adopted from earlier research, while the stress-strain relationship for FRP reinforcement was established experimentally.

Moment-curvature relationships were computed by plane-section analysis, as described above, and were plotted for comparison with experimentally obtained relationships. Hognestad's concrete model (1955) was used for cover concrete and Saatcioglu and Razvi confinement model (1992) was used for core concrete. Concrete strength in member was assumed to be the same as that obtained by standard cylinder tests. Experimental curvatures were obtained based on the LVDT readings were instrumented within the potential plastic hinge region. The gauge length for LVDTs was equal to 405 mm (equal to the beam dimension in the direction of loading), which gave total rotation. Another LVDT was placed at 25 mm above the footing to provide the rotation of the beam base section, which caused by anchorage slip (elastic extension of FRP bars within the column). The

[Downloaded from ijce.iust.ac.ir on 2024-07-23]

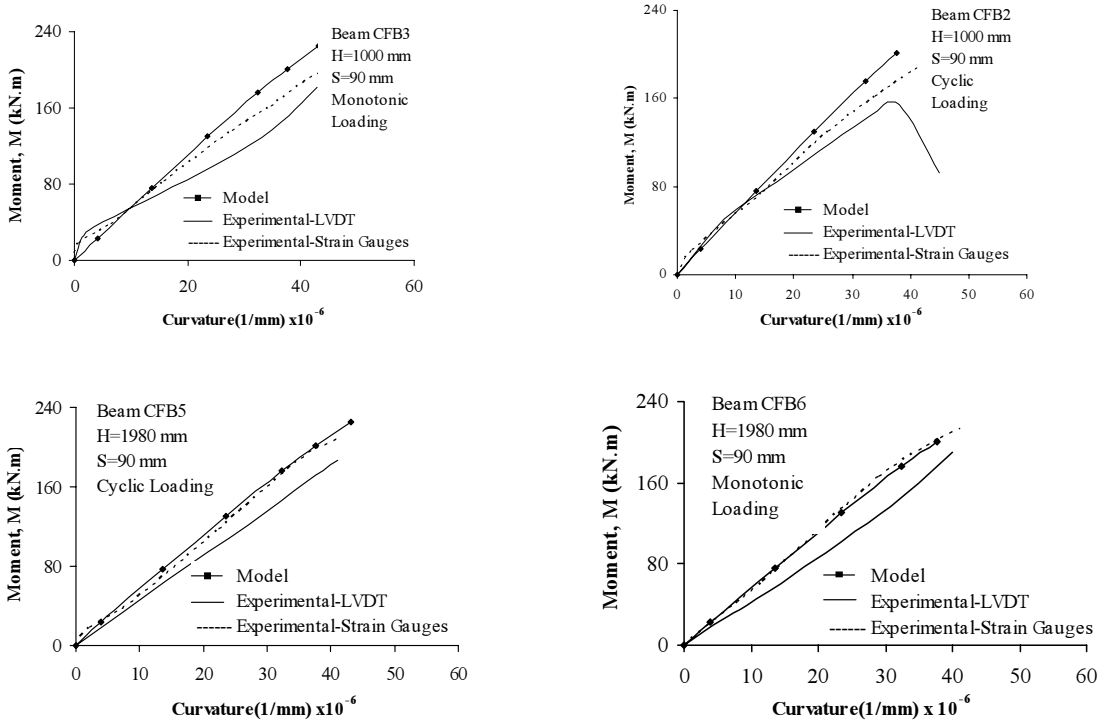

Fig.13 Moment-Curvature Diagrams of Beams

difference between measured total rotation and anchorage slip gave flexural rotation within 355 mm of column segment. The flexural rotation divided by the segment length provided experimental average curvature to be plotted against average moment within the 355 mm segment for comparison with analytical moment-curvature relationship. The comparison for each beam is illustrated in Figures 13. The figure also includes a second set of relationships for experimental moment-curvature relationships, this time obtained from the strain gauges located on longitudinal FRP bars at column-footing interface. These relationships show curvatures and corresponding moments at exactly the beam-column interface.

The results indicate approximately linear moment-curvature relationship for both analytical and experimental values because of the failure mode of beams. All beams failed by rupturing of FRP bars in tension before crushing of concrete. Maximum compressive fiber strain recorded was approximately 0.003, which is only slightly above the strain at unconfined concrete strength. The agreement between analytical and experimental values is reasonably good, once again confirming the applicability of plane section analysis to FRP reinforced concrete beams.

5. Summary And Conclusion

Experimental and analytical results of beam tests conducted in this paper present several conclusions. Tension FRP reinforcement would rupture prior to significant distress in concrete at all beams except for CFB1, which was critical in shear. And also all the flexure dominant beams developed their flexural capacities computed on the basis of plane-strain analysis. Beams with short shear span and wide spacing of transverse reinforcement developed a wide diagonal tension crack due to shear, resulting in diagonal tension failure in tensile bars, while the compression bars were subjected increased dowel action in addition to compression, and experienced stability failure and then was broke. Beams with the same grid spacing but long shear span were able to develop

[Downloaded from ijce.iust.ac.ir on 2024-07-23]

their flexural strength without shear failure, resulting in rupturing of FRP bars in tension.

The results also indicate that the force-deformation relationships obtained under monotonically increasing lateral force are similar to the envelopes of hysteretic relationships obtained under reversed cyclic loading, suggesting very little or no effect of cyclic loading on beams and this implies that a monotonic curve would provide sufficient strength envelope for hysteretic relationships of FRP reinforced beams. The hysteretic relationship of flexure dominant FRP reinforced beams indicate stiffness degradation under cyclic loading, due to progressive cracking of concrete and associated softening in the member, developing approximately 3% lateral drift ratio prior to failure. This level of lateral drift may be considered to be sufficient for earthquake resistant construction. Moreover the results indicate approximately linear moment-curvature relationship for both analytical and experimental values because of the failure mode of beams by rupturing of FRP bars in tension before crushing of concrete. The agreement between analytical and experimental values is reasonably good, confirming the applicability of plane section analysis to FRP reinforced concrete beams.

6. Acknowledge

The author would like to acknowledge Professor Murat Saatcioglu (U of Ottawa) for his guidance, valuable suggestions, encouragement, and funding and also Technical officers of the Structural Laboratory at the University of Ottawa in Canada for their assistance and continuous support during the course of this investigation.

7. Reference

[1] ACI Committee 318, 1999. Building code requirements for reinforced concrete and commentary (ACI 318-95). American Concrete Institute, Farmington Hills, MI. 369 pp.

[2] ACI Committee 440(1999), "Provisional Design Recommendations for Concrete Reinforced with FRP Bars", American Concrete Institute, USA.

[3] ACI Committee 440 (1996), "State-of-Art report on Fiber Reinforced Plastic Reinforcement for Concrete Structures," American Concrete Institute, USA, 1996,68 pp.

[4] ACI Committee 440.1R-01(2001), "Guide for the Design and Construction of Concrete Reinforced with FRP Bars", American Concrete Institute, USA, 2001, 41 pp.

[5] ACMBS III, Advanced Composite Materials in Bridges and Structures.(2000). "Proceedings of the Third International Conference (Ottawa, Canada)". Humar, J., and Razaqpur, G. editors. The Canadian Society for Civil Engineering, Montreal, Canada.

[6] Alsayed, S.H., Al-Salloum, Y. A., Almusallam, T.H., and Amjad, M. A. (1999). "Concrete Columns Reinforced by Glass Fiber Reinforced Polymer Rods," American Concrete Institute, Special Publication, SP-188, Farmington Hills, Michigan, p.103-112.

[7] Canadian Standards Association, S806-02, May 2002, " Design and Construction of Building Components with Fibre-Reinforced Polymers", CSA, Ontario.

[8] FRPRCS-3, Non-Metallic Reinforcement for Concrete Structures. (1997). "Proceedings of the Third International Symposium on Non-metallic (FRP) reinforcement for Concrete Structures (Sapporo, Japan)". Japan Concrete Institute, Tokyo, Japan.

[9] FRPRCS-4, Fiber Reinforced Polymer Reinforcement for Concrete Structures. (1999). "Proceedings of the Fourth

[Downloaded from ijce.iust.ac.ir on 2024-07-23]

International Symposium (Baltimore, USA)". Dolan, C. W., Rizkalla, S.H., and Nanni, A. editors. SP-188, American Concrete Institute,

[10] Fukuyama, H. and Masuda, Y. (1995). "Structural Performances of Concrete Frame Reinforced with FRP Reinforcement," Non-metallic (FRP) Reinfocement for Concrete Structures. Edited by Taerwe. E&FN Spon, London, p.275-286.

[11] ISIS Canada, ISIS-M04-00 Draft, 2000, " Reinforcing Concrete Structures With Fibre Reinforced Polymers", Manitoba, Winnipeg, Canada.

[12] Japanese Society of Civil Engineers (JSCE). (1997). "Recommendation for Design and Construction of Concrete Structures Using Continuous Fiber Reinforcing Materials." Concrete Engineering Series 23.Tokyo.

[13] J.G.Teng, J.F.Chen, S.T.Smith, L.Lam (2002), " FRP Strengthened RC Structures", John Wiley&Sons Ltd.

[14] Kent D.C. and Park R. (1971), " Flexural Members with Confined Concere," Journal of Structural Division, ASCE, 97(ST7), p.1969-1990.

[15] Kobayashi, K. and Fujisaki, T. (1995). "Compressive Behavior of FRP Reinforcement in Non-Prestressed Concrete Members," Non-metallic (FRP) Reinfocement for Concrete Structures. Edited by Taerwe. E&FN Spon, London, p.267-274.

[16] Mongi Grira, " Innovative Approaches to Column Confinement", PhD Thesis, University of Ottawa,1998.

[17] Nagasaki T, Fukuyama H, and Tanigaki M, " Shear Performance of Concrete Beams Reinforced with FRP Stirrups," 1993, ACI, SP-138-47, p.789-811.

[18] Nanni, A.(2001)," North America design Guidelines for Concrete Reinforcement and Strengthening Using FRP: Principles, Applications, and Unresolved Issues" FRP Composites in Civil Engineering,Vol1, Conference proceeding, Hong Kong,2001.

[19] Pauly, T., Priestly, M.J.N., " Seismic Design of Reinforced Concrete and Masonry Buildings", Jihn Willey & Sons, New York, 1991, 744 pp.

[20] Saatcioglu, M., and Salamat, A.H., and razvi, S.R., "Confined Columns Under Eccentric Loading," Journal of Structural Engineering, ASCE, 1995, 121(11), p.1547-1556.

[21] Sameh R. Salib et al (2001)," Strength of Concrete Beams Reinforced and/or Prestressed With FRP Bars", FRP Composites in Civil Engineering,Vol1, Conference proceeding, Hong Kong,2001.

[22] Sonobe, Y., Fukuyama, H., Okamoto, T., Kani, N., Kimura, K., Kobayashi, K., Masuda, Y., Matsuzaki, Y., Mochizuki, S., Nagasaka, T., Shimizu, A., Tanao, H., Tanigaki, M., Teshigawara, M. (1997). "Design Guidelines of FRP Reinforced Concrete Building Structures." Journal of Composites for Construction, ASCE, Vol. 1, No.3,90-114.

[Downloaded from ijce.iust.ac.ir on 2024-07-23]